Topology Insensitive Location Determination Using Independent Estimates Through Semi-Directional Antennas

Chin-Lung Yang, Saurabh Bagchi, and William J. Chappell, *Member, IEEE*

***Abstract*—We demonstrate the effect of using multiple estimations from independent single wireless motes in order to decrease network topology dependence on location estimation in a wireless sensor network. A method of determining the location of a target by using multiple compact semi-directional antennas is shown to give an independent estimate of location from each sensor mote in a network, each estimate not relying on the data from neighboring motes as in the case of traditional triangulation. We begin by demonstrating a method of using angular diversity through multiple semi-directional antennas in order to ascertain the location of a target. The estimation of both range and angle is demonstrated in the presence of a noisy and/or faded channel. An efficient and fast algorithm on a wireless sensor mote is presented through a Taylor series expansion of the simulated antenna pattern. Furthermore, using the results from the location estimation from a single node, location determination in a realistic network is explored through both theory and simulation. The results indicate that our proposed algorithm depends significantly less on the topology (spatial arrangement) of the anchor nodes. While network planning for a variety of topologies of anchor nodes is shown to be necessary when using triangulation, our proposed algorithm is insensitive to the deployments of the anchor nodes. A testbed was created in order to experimentally demonstrate that the predictions are accurate even in triangulation-adverse topologies. The experimental testbed shows that a linear arrangement of closely spaced sensors can reduce the location error to one-fourth of the location error using triangulation.**

***Index Terms*—Directional antennas, location determination, sensor networks, topology, triangulation.**

I. Introduction

WIRELESS sensor networks have been drawing increased attention due to their widespread applications in a variety of civilian and military applications. Tiny and cheap wireless nodes equipped with different kinds of sensors can be placed in the area of interest to monitor conditions and collect information. Both temporally and spatially varying information of an event can be obtained to gather a more informative collection of data. Location determination is essential to many sensor networks because most sensor information can only be meaningful by knowing the location of the source of data. For some applications, such as battlefield monitoring and data gathering from remote locations [1], sensor networks can be mobile in nature. Therefore, accurate real time location estimation of a dynamic system is important.

However, expensive and comprehensive solutions are contrary to the purpose of the wireless sensor network because wireless sensor nodes have strict hardware and software restrictions including limited size, data, instruction memory, storage, computational power, and power consumption. A dynamic network configuration can be efficiently created with the assistance of the position information to optimize the routing process as in many position-aware routing protocols [2]. Overall, position awareness is often an essential requirement in sensor networks, either from the communication aspects or the sensor data gathering.

It is important from the point of scaling up the network that the deployment is relatively easy. This implies that the location determination protocol is desirable to not enforce a rigid topology of the network vis-à-vis the placement of a given node with respect to other nodes. Our proposed protocol is less sensitive to topology than the prevalent triangulation based techniques. While the algorithms and concept are specifically developed for and tested on a sensor network, our approach is generically applicable to any wireless network which might require localization.

There are three distinct techniques used to determine relative position with respect to a neighbor node: angle-of-arrival (AOA), received signal strength (RSS), and propagation-time methods such as time-of-flight [3]. After knowing the relative positions from multiple neighbors, triangulation-based techniques are applied to determine the location [4]. Alternately, connectivity information may be used to determine coarse-grained position information [5].

In AOA systems, the position is calculated via angulation with the use of highly directional antennas or antenna arrays. However, the large cost and size of these antennas typically eliminates them from large scale sensor network applications and makes this approach suitable for base stations instead of tiny sensor nodes. The high directionality implies impractically large radiator. Applying radio wave propagation-time based approaches is difficult in wireless sensor networks because the

Manuscript received December 16, 2005; revised May 19, 2006. This work was supported in part by the National Science Foundation under Grant ECS-0330016.

C.-L. Yang is with the Center for Wireless Systems and Applications, Electrical and Computer Engineering Department, Purdue University, West Lafayette, IN 47907 USA (e-mail: cyang@purdue.edu).

S. Bagchi is with the Dependable Computing Systems Lab, Center for Wireless Systems and Applications, Electrical and Computer Engineering Department, Purdue University, 465 Northwestern Avenue, West Lafayette, IN 47907 USA (e-mail: sbagchi@purdue.edu).

W. J. Chappell is with the Birck Nanotechnology Center and the Center for Wireless Systems and Applications, Electrical and Computer Engineering Department, Purdue University, West Lafayette, IN 47907 USA (e-mail: chappell@purdue.edu).

Color versions of Figs. 1–15 are available online at http://ieeexplore.ieee.org.

Digital Object Identifier 10.1109/TAP.2006.884294

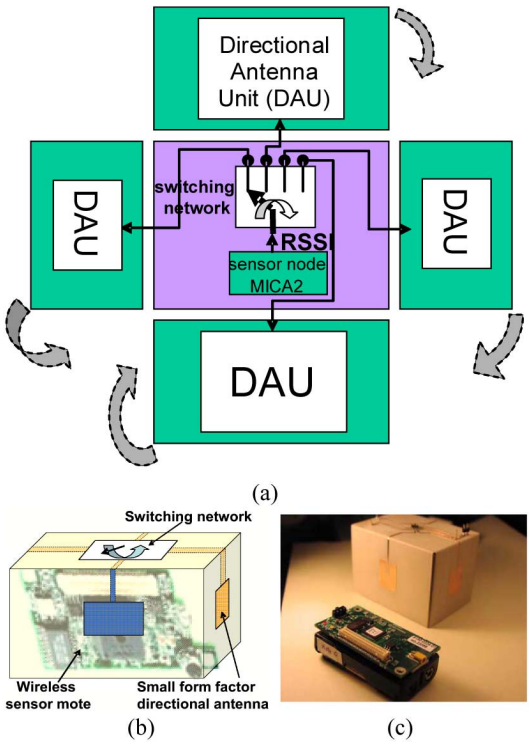

Fig. 1. (a) System diagram of the motes using multiple directional antennas; (b) a single mote with angular antennas controlled by a switch; (c) wireless sensor node and makeup of test node.

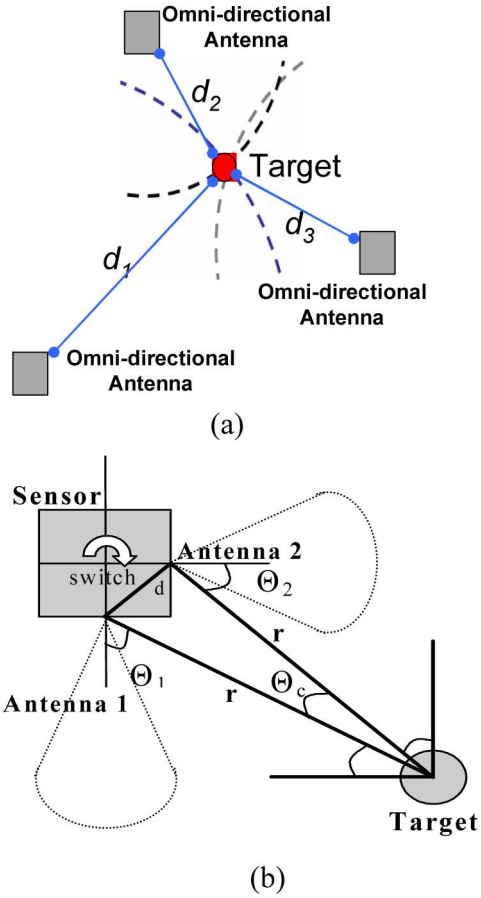

Fig. 2. Comparison of traditional versus proposed localization techniques. (a) Traditional location determination using triangulation with three omnidirectional transmitters and an omnidirectional receiver; (b) Proposed location determination with an omnidirectional transmitter and directional receiver.

traveling time of the radio signal between sensor nodes is relatively short. A positioning accuracy in the meter range requires an absolute time resolution significantly below 100 ns. Therefore, this technique is not preferred in wireless sensor nodes because of hardware complexity.

RSS systems are based on measuring the propagation loss with distance. The received power of the signal from the neighbor is measured by the sensor node. The signal strength emitted by the neighbor and the attenuation relation of the signal with distance are known, so the relative distance can be calculated. This system is applicable to sensor networks because the radio modules on the nodes (e.g., the Mica motes [6]) provide a received signal strength indicator, RSSI, and hence no additional hardware is needed. However, in practice the exact nature of the signal propagation loss with distance is unknown; therefore, the scheme entails error in location computation, which can be estimated through statistical techniques [7]. Measurements from multiple nodes need to be coordinated to refine the location estimation error, and those results will be discussed in this paper.

With omnidirectional antennas, a distance can be estimated from a single node but only with 360 degrees of ambiguity, so standard triangulation techniques are required [see Fig. 2(a)]. In this paper, a novel algorithm for location determination based on combining RSS and AOA is proposed with compact semi-directional antennas, but with relatively low complexity of computation and low cost of implementation. A means to realize the sensor nodes with directional antennas is shown in Fig. 1. Furthermore, triangulation techniques are not required and each estimate is not dependent on the neighboring nodes. The independence of estimations greatly decreases the sensitivity of the multiple measurements and the topology of the network. The approach is demonstrated through implementation and experimentation using a specific type of sensor nodes—the Crossbow Mica motes [6]. The directionality is realized by low cost patch antennas; however any type of directional antennas could be used, as long as the pattern is known. In addition, independent of the location estimation technique, directional antennas can provide important benefits in sensor networks such as increasing the communication range, providing angular information, angular channel diversity, and interference suppression. Therefore, overall networking performance enhancement would be expected in system-level aspect.

Though it may be very costly for all nodes to be equipped with location determination hardware, it may be possible to equip a small fraction of the nodes in the network with such hardware, or the location of these nodes can be noted on deployment and other motes will be referenced to these known locations. A relative coordination is thereby established. The proposed system has two kinds of wireless sensor nodes. *Anchor motes*, which know their location by noting the location upon deployment or through assistance with sophisticated equipment

such as GPS, act as reference points for determining the locations of other nodes, which are called *target motes*. The anchor motes are equipped with multiple directional antennas with a switch between them that is capable of switching among the antennas for transmitting or receiving (see Fig. 2). In our scheme, the antennas need not be highly directional, though the accuracy of the scheme improves with higher directivity.

The location estimation algorithm can be independently solved on the anchor mote by comparing the received signals from the multiple antennas of one target mote, and then refined by averaging the independent estimates over all the neighboring anchor motes. So the computational complexity of executing our algorithm has linear growth with the density of the network, instead of $O(N^3)$ when solving using triangulation. Furthermore, the dependence on the topology of the anchor motes is reduced, where the topology means the relative spatial arrangement of the anchor motes. Our proposed system has the merits of low memory storage and computational time requirements for the algorithm, low energy consumption, predictable error distribution based on the channel model estimation, decentralization of location determination, slow growth of error with inter-node distances and insensitivity to network topology. Equally as important, this location scheme does not require any expensive hardware upgrades on the motes since a single switch and the multiple antennas are relatively inexpensive, allowing for deployment of the hardware upgrades to the most to be widespread throughout the network.

This paper is organized as follows. The new location detection algorithm for independent estimation is described in Section II. The ability of a single mote to do location determination on its own is presented in Section III. The net effect of independent location estimate on the location estimation in a network is presented in Section IV. The results and discussions are given in Section V. Finally, conclusions on the feasibility and the merits of these techniques are drawn, indicating that this is a viable approach.

II. New Location Detection Algorithm

The solution to location determination using triangulation with omnidirectional antennas is *not* applicable to directional antennas, because the received power depends on angle of transmission and reception as well as the distance. Directionality provides relative angle measurements between anchor motes and target motes with unknown positions and has been argued to improve localization estimates [8], [9]. In this section, we demonstrate an accurate, topology insensitive location determination method using knowledge of the angle of reception in a single mote.

Based on the measurements of received signal strengths, distance between anchor and target motes can be determined by the path-loss relation. There are two major methods to determine the path-loss. The first method is to build up a map of signal strength and position in a physical space using off-line data collection such as in RADAR [10]. However, this could take much effort in a large field. The second is applying the model-based path-loss equations [11]. Both of these are known to be only partially accurate and an algorithm that is insensitive to path loss estimations is desired. For the simplest case, the received power at a directional antenna in free space is given by Friis' formula (1)

$$P_r = \frac{P_t G_t(\Theta_t) G_r(\Theta_r)}{r^2} \left(\frac{\lambda}{4\pi}\right)^2 \tag{1}$$

where, P_t and P_r are the transmitted and the received powers, respectively. $G_t()$ and $G_r()$ are the gain functions of the transmitting and receiving antennas, Θ_t and Θ_r are the transmitting and the receiving angles, and r is the distance between the transmitter and the receiver. The radiation patterns can be obtained from the numerical simulations such as Ansoft HFSS™ according to the patch geometry and further verified from measurements. In our anechoic chamber measurement, the radiation patterns of measurements and simulations are close (within 5.7%) [9], so either the simulation or the measured data can be used for the algorithm interchangeably. The simulated patterns are applied in order to obtain a finer angular resolution, but interpolation or more detailed measurements could be utilized. For ease of presentation, the constant $(\lambda/4\pi)^2$ and other system constant terms, such as antenna efficiency and system loss which can be determined in advance and shown in Section III-A, overall regarded as assumed overall system constant, will be excluded from future equations, though they are used in the actual calculations.

Friis' formula is based on the assumption that there is no multipath effect and no noise. In practice, multipath, noise, and measurement errors will induce errors in the distance calculation, the extent of which will be explored in the experimental sections. Since errors are not cumulative for the network, this approximation is shown to be appropriate for our calculations, as verified through measurements. Our approach is not limited to environments where the Friis' formula holds. Rather, it can be generically applied with other complex path loss statistical models, possibly generated through empirical measurements to improve the accuracy. For instance, a simulation-based Ray-tracing model can be applied for site specific applications [12] or a practical path loss model can be modified empirically for general applications and environments considering the physical factors [13], [19], however this is not shown herein. The application of Friis formula is shown to be appropriate through the results gathered and so the dependence on this approximation is appropriate.

A. Basic Formula of Location Estimation

Single anchor—In this section, we will demonstrate how an independent estimate of location can be determined on a single target mote through the use of directional antennas. Anchor motes with four directional antennas receive signals from target motes with omnidirectional antennas to determine the location of the target. Let $P_{r,i}$ denote the power received by antenna i on the anchor mote. From the geometric constraints on Θ_1, Θ_2, and Θ_c from Fig. 2, the fundamental set of equations with three unknowns is shown as follows:

$$\begin{aligned} P_{r,1} &= \frac{P_t}{r^2} G_t G_r(\Theta_1) \\ P_{r,2} &= \frac{P_t}{r^2} G_t G_r(\Theta_2) \\ \Theta_2 &= \Theta_1 - \Theta_c - \frac{\pi}{2}. \end{aligned} \tag{2}$$

Since these are nonlinear equations, a closed form solution for Θ_1, Θ_2, and r is difficult to compute in terms of the input variables $P_{r,1}$ and $P_{r,2}$. Therefore, offline numerical methods can be used to solve the equations, such as using MATLAB which was used for the initial calculations in our testbed [14]. However, this offline computation is not applicable on motes in a real application, so a simple and direct solution is desired on sensor network applications.

When $r >> d$ where d is the distance between the centers of two adjacent patch antennas, we can reasonably approximate that $\Theta_c = d/r$. This is appropriate since Θ_c is less than 0.1 (rad) if r is larger than 0.6 meters and the approximation works for small angles as will be experimentally demonstrated in Section III-C. After some rearrangements of (2) and approximating d to 0, an analytic form of the solution to the estimated position can be obtained as follows:

$$\hat{\Theta}_1 = G_{\text{diff}}^{-1}\left(\frac{P_{r,1}}{P_{r,2}}\right) \tag{3}$$

$$\hat{r} = \left(\frac{P_t G_t G_r(\hat{\Theta}_1)}{P_{r,1}}\right)^{1/2} \tag{4}$$

where G'_{diff} is the inverse function of $G_r(\Theta)/G_r(\Theta - \pi/2)$ and $\hat{\Theta}_2$ is the same as in (2). The assumed overall system constant is factored out in (3), so angular estimation reduces the dependence on this constant. Note that these are estimates of the actual values due to the approximation introduced by the use of the Friis' formula. Equation (3) gives us an intuitive interpretation that $\hat{\Theta}_1$ is related to the difference of the received power strengths from two adjacent antennas. Once the angle is estimated, the range estimation can be determined by (4).

Since we know the distance as well as the relative direction of the target with respect to the anchor, the relative location between the target and the anchor motes can be calculated at the receiving motes (either target or anchor motes). This estimate is based on measurements at just one neighboring anchor mote whereas triangulation requires measurements from at least three. Therefore this algorithm using direct, one-to-one solution is efficient and fast. Though this closed form formula is derived by neglecting small Θ_c (and consequently d), numerical analysis, detailed in Section III-C, shows that the location error results are close to the results considering Θ_c.

Multiple anchors—While a location estimate using a single anchor mote is possible, additional estimations can be combined to obtain a more accurate location determination while maintaining linear complexity [9]. Here the target mote is estimating its location based on received signal strengths from multiple anchor motes. In other approaches to improve location estimate by using multiple anchor motes, the communication becomes much more complicated due to overhead of information exchange, and simultaneously solving multiple non-linear equations costs much more computation power. Based on estimating the target position individually, a simple, efficient aggregate estimation scheme from multiple anchor motes is proposed with the same complexity as that of the individual estimation.

Traditional triangulation needs to function with at least three anchor motes as a minimal requirement. As the number of anchor motes increases, the location estimation algorithm uses the least square method to determine the positions. This requires solving the inverse of a matrix whose dimension is the number of the anchor motes, and hence has computational complexity $O(N^3)$ [15], [16].

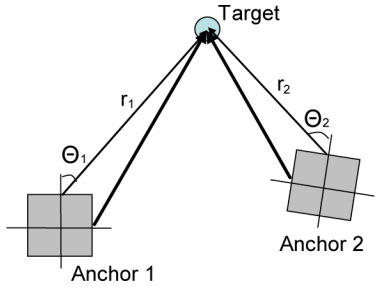

Fig. 3. Deployment of multiple anchor motes with directional antennas for location determination.

Using the scheme presented for the single anchor, an independent estimate is obtained from each anchor then averaged over all anchor motes in communication range with proper weights. For the simplest case, equal weights (see Fig. 3) are used

$$(\hat{x}_i, \hat{y}_i) = \hat{r}_i \times (\cos(\hat{\Theta}_i), \sin(\hat{\Theta}_i)) + (x_{i,0}, y_{i,0})$$
$$(\hat{x}, \hat{y}) = \frac{1}{M}\sum_i (\hat{x}_i, \hat{y}_i). \tag{5}$$

In this equation, $(x_{i,0}, y_{i,0})$ is the known position of anchor i and M is the number of the anchor motes. As the M increases, the location error reduces, and convergence of this term has been shown [9]. The complexity of the scheme is proportional to the number of anchor motes in communication range of the target mote. Though triangulation can also utilize averaging to reduce the complexity with sacrifice of the performance, however, our proposed method of low complexity still outperforms the triangulation of high complexity (in Section IV). Furthermore, the protocol design is simple since there is no need to coordinate between the anchor motes eliminating network overhead. Therefore, the scheme is scalable to large wireless sensor networks.

B. Stochastic Model of Location Estimation

Since the channel conditions vary depending on space and, to a limited extent, time, therefore the deterministic set of (3)–(5) cannot be used to solve for the angle and the distance in the entire network. Therefore, stochastic modeling is needed to provide the probability distribution of the estimated range r and angle Θ. In this context the existence and the uniqueness of the distributions is also important. From this, the error distribution for the estimates can be extracted. In this section, we present such a model and the accompanying analysis. We use the Rician distribution for the received power as an approximation in the line-of-sight (LOS) case and the Rayleigh distribution in the non-LOS case, where the variability of the received signal is higher and the error in location estimation is consequently higher. Our methodology can be applied to the more general model with Nakagami pdf or two-wave incoherent power (TIP) pdf [17], which subsumes the Rayleigh and the Rician models. In the outdoor environment, the Rician model is typically used and the Rayleigh model is used to derive the worst case behavior. The use of the Rician distribution is reasonable

because the inter-node distances are not too large. Other signals from scatterers are assumed to arrive from all possible angles. In our analysis, we assume that the signal to interference ratio of the channel model stays constant through the field of interest, though the dominant signal strength receiving by different directional antennas may vary due to the orientations of the antennas.

Equations (3) and (4) do not guarantee the uniqueness and the existence of the solutions when $P_{r,1}$ and $P_{r,2}$ vary due to a fading channel. The uniqueness of the solution can only be obtained by eliminating some solutions based on domain knowledge of how directional antennas are set up. For our testbed example, the ranges of Θ are restricted to $[-79, 160]$ (this range can be numerically determined in Section III-D). This constraint is reasonable because of the nature of the directional antennas in use.

If the exact solution turns out to be infeasible, then an optimization method is used to obtain the solution with the least error from (2)

$$f_{\text{error}} = \min_{\Theta_1,\Theta_2,r} \left\{ \left(\left(\frac{P_t}{r^2} G_t G_r(\Theta_1) \right)_{\text{dB}} - P_{r,1,\text{dB}} \right)^2 + \left(\left(\frac{P_t}{r^2} G_t G_r(\Theta_2) \right)_{\text{dB}} - P_{r,2,\text{dB}} \right)^2 \right\}, \quad \text{s.t.} \hat{\Theta}_2 = \hat{\Theta}_1 - \frac{\pi}{2} - \frac{d}{\hat{r}}. \quad (6)$$

The intuition behind this is simple. The positions are estimated by minimizing the sum of square of errors between predicted received power (from the model) and the actual received power, subject to geometry constraints. According to optimization theory, the minimal solution occurs at $\partial f_{\text{error}}/\partial r = 0, \partial f_{\text{error}}/\partial \Theta = 0$ [18]; where f_{error} is the object function in (6). Therefore, after some manipulation, an analytic form of the optimum solution can be obtained as follows (see Appendix I-A):

$$\hat{\Theta}_1 = \begin{cases} G_{\text{diff}}^{-1}\left(\frac{P_{r,1}}{P_{r,2}}\right), & \text{or} \quad (7.a) \\ \max\left\{G_{\text{diff}}^{-1}\left(\frac{P_{r,1}}{P_{r,2}}\right)\right\} & \left(\text{when} \frac{P_{r,1}}{P_{r,2}} \gg 1\right) \quad (7.b) \\ \min\left\{G_{\text{diff}}^{-1}\left(\frac{P_{r,1}}{P_{r,2}}\right)\right\} & \left(\text{when} \frac{P_{r,1}}{P_{r,2}} \ll 1\right) \quad (7.c) \end{cases}$$

$$\hat{r} = \left(\frac{P_t^2 G_t^2 G_r(\hat{\Theta}_1) G_r(\hat{\Theta}_2)}{P_{r,1} P_{r,2}} \right)^{1/4}. \quad (8)$$

(7.a) is the same as (3), but when the received power difference is out of the domain range of $G'_{\text{diff}}()$ function, (7.b) and (7.c) show that the optimal angle estimation occurs at the boundary. From (8), the best estimation of the range is obtained from the geometric mean of the range estimations from individual directional antennas by (3) and (4). $P_{r,1}$ and $P_{r,2}$, the received power on two adjacent directional antennas, are assumed to be independent. This assumption holds true in outdoor environments where the correlation less than 10% in our experimental testbed (Section III). Assume *a priori* probability distributions ($f_{Pr,1}$ and $f_{Pr,2}$) of $Pr, 1$ and $Pr, 2$ are known, and variable transformations of square law ($Y = X^2$, where X denotes envelopes of voltages v_1, v_2 and Y denotes powers $P_{r,1}, P_{r,2}$) from the Rician distributions of (v_1, v_2) are performed respectively. The estimated range $\hat{r}$ and angular $\hat{\Theta}_1$ will be random variables (r.v.) following the joint distribution by Jacobian variable replacement as shown in (9)

$$\begin{aligned} f_{R,\Theta}(r,\theta) &= f_{P_{r,1}}(p_{r,1} = f_1(r,\theta)) \\ &\quad \times f_{P_{r,2}}(p_{r,2} = f_2(r,\theta)) \left| \frac{\partial p_{r,1} \partial p_{r,2}}{\partial r \partial \theta} \right| \\ &= f_{P_{r,1}}\left(p_{r,1} = \frac{P_t G_t G_r(\theta)}{r^2}\right) \\ &\quad \times f_{P_{r,2}}\left(p_{r,2} = \frac{P_t G_t G_r(\theta - \pi/2)}{r^2}\right) \\ &\quad \times \left| \frac{G_r(\theta) G_r'(\theta - \pi/2) - G_r'(\theta) G_r(\theta - \pi/2)}{R} \right|. \end{aligned} \quad (9)$$

The joint distribution $f_{R,\Theta}$ can be pre-calculated, and the variance of location estimation errors can be obtained, so this location error table can be stored in the motes [6]. We use numerical calculation to show the joint distribution of the two estimated parameters—range and angle estimates—in Section III, and compare with the range estimation using omnidirectional antenna to show that using directional antenna provides more accurate range estimation in theory. With this stochastic model, the location error distribution can be obtained for realistic, time-varying received signals.

C. Stochastic Model With Additive Gaussian Noise and Measurement Errors

For a wireless channel, the additive noise such as thermal noise from channel or receivers and the measurement errors are also important factors possibly degrading the performance of the location estimation. In this section, an analytic model with noise and measurement errors is created and simulations are applied to verify this model in Section III-E. Equation (2) is modified to include a Gaussian random variable, n_i describing noise at the receiver

$$\frac{P_t}{r^2} G_t G_r(\Theta_i) = P_{r,i}^{'} o; \quad i = 1, 2 \quad (10.a)$$

$$P_{r,1}^{'} = P_{r,1} + n_1^2; \quad P_{r,2}^{'} = P_{r,2} + n_2^2 \quad (10.b)$$

where $P_{r,1}$ and $P_{r,2}$ are deterministic. $P_{r,1}^{'}$ and $P_{r,2}^{'}$ are expected received powers including noise, and n_1 and n_2 are independent Gaussian random variables with zero mean and variance of the noise power. To estimate the angular and range variance caused by noise, similar analysis from previous section is processed by applying (10.a) and (10.b) into (6). Therefore, (7) and (8) can be applied with replacement of $P_{r,1}$ by $P_{r,1}^{'}$ with (10.b). For simplicity, we consider only case (7.a) and neglect the extreme cases (7.b) and (7.c) which rarely happen if the signal-to-noise ratio (SNR) is not too small. For example, when the $\text{SNR} > 0$, the probability of these two extreme cases occurs less then $5 \bullet 10^{-6}$, so the conditions described by (7.a) is the most important

$$\hat{\Theta}_1 = G_{\text{diff}}^{-1}\left(\frac{P_{r,1}^{'}}{P_{r,2}^{'}}\right) \approx \sum_{i=1}^{\tilde{N}} c_i \left(\frac{P_{r,1} + n_1^2}{P_{r,2} + n_2^2}\right)^i \quad (11)$$

where c_i's are coefficients of a polynomial Taylor series expansion to approximate the function G_{diff}^{-1} from (3), and $\tilde{N}$ is the order of truncated polynomial. Considering the case of $P_{r,2} >$

$P_{r,1}$ (to estimate the angular errors from 0 to 45 degrees), the angular estimation variance can be approximated numerically as (12.a) which is simply the variance of polynomial of one Gaussian r.v.—from 45 to 90 degrees, similar results can be obtained. Using the symmetry property due to the switching mechanism, the overall variance can be sufficiently calculated from 0 to 90 in (12.b).

$$\begin{aligned}&\operatorname{var}\left(\hat{\Theta}_1 \,|\, P_{r,2} > P_{r,1}\right)\\ &\quad\approx \operatorname{var}\left(\sum_{i=1}^{\tilde{N}} c_i \left(\frac{P_{r,1}+n_1^2}{P_{r,2}}\right)^i\right) \qquad (12.a)\\ &\operatorname{var}(\hat{\Theta}_1)\\ &\quad\approx \frac{1}{2}\operatorname{var}\left(\sum_{i=1}^{\tilde{N}} c_i \left(\frac{P_{r,1}+n_1^2}{P_{r,2}}\right)^i\right)\\ &\qquad+\frac{1}{2}\operatorname{var}\left(\sum_{i=1}^{\tilde{N}} c_i \left(\frac{P_{r,1}}{P_{r,2}+n_2^2}\right)^i\right). \qquad (12.b)\end{aligned}$$

Similarly, the variance of range can be evaluated in the same method numerically (in Appendix.B). The joint distribution of $\hat{r}$ and $\hat{\Theta}(f_{R,\Theta})$ can be obtained by Jacobian variable replacement, which is shown in Appendix.B. This joint pdf predicts the location error distribution when noise exists and can be compared with (9). For simplicity, the variance of joint distributions (9) and (B.3) are calculated to compare the influences of these two kinds of random error sources.

Besides the random noise, systematic variations such as RSSI measurement errors result in location estimation errors as well. Instead of modeling individual RSSI errors from $P_{r,1}$ and $P_{r,2}$, the error of the ratio $P_{r,1}/P_{r,2}$ is assumed to be weighted by a random variable A_{RSSI}, because the angular estimation is a function of $P_{r,1}/P_{r,2}$. For simplicity, A_{RSSI} is assumed to follow a uniform distribution:

$$\begin{aligned}&\hat{\Theta}_1\\ &\quad= G_{\mathrm{diff}}^{-1}\left(\left(A_{\mathrm{RSSI}}\frac{P_{r1}}{P_{r2}}\right)_{\mathrm{dB}}\right);\\ &\qquad A_{\mathrm{RSSI,dB}} : U(-A_{\mathrm{RSSI,max}}, A_{\mathrm{RSSI,max}}) \qquad (13)\\ &\operatorname{var}(\hat{\Theta}_1)\\ &\quad= \operatorname{var}\left(E\left\{G_{\mathrm{diff}}^{-1}\left(A_{\mathrm{RSSI}}\frac{P_{r1}}{P_{r2}}\right)\,\middle|\, P_{r1}, P_{r2}\right\}\right)\\ &\qquad+E\left\{\operatorname{var}\left(G_{\mathrm{diff}}^{-1}\left(A_{\mathrm{RSSI}}\frac{P_{r1}}{P_{r2}}\right)\,\middle|\, P_{r1}, P_{r2}\right)\right\}\\ &\quad> E\left\{\operatorname{var}\left(G_{\mathrm{diff}}^{-1}\left(A_{\mathrm{RSSI}}\frac{P_{r1}}{P_{r2}}\right)\,\middle|\, P_{r1}, P_{r2}\right)\right\}\\ &\quad= \int\left\{\int_{A_{\mathrm{RSSI,min}}}^{A_{\mathrm{RSSI,max}}}\frac{\left(\sum_{i=1}^{\tilde{N}} c_i(a_{\mathrm{RSSI}}p_{\mathrm{dif}}f)^i\right)^2}{A_{\mathrm{RSSI,max}}-A_{\mathrm{RSSI,min}}}da_{\mathrm{RSSI}}\right.\\ &\qquad\left.-\left(\int_{A_{\mathrm{RSSI,min}}}^{A_{\mathrm{RSSI,max}}}\frac{\sum_{i=1}^{\tilde{N}} c_i(a_{\mathrm{RSSI}}p_{\mathrm{dif}})^i}{A_{\mathrm{RSSI,max}}-A_{\mathrm{RSSI,min}}}da_{\mathrm{RSSI}}\right)^2\right\}\\ &\qquad\times f_{P_{\mathrm{DIF}}}(p_{\mathrm{dif}})dp_{\mathrm{dif}} \qquad (14)\end{aligned}$$

where P_{DIF} denotes a r.v. of $P_{r,1}/P_{r,2}$ where target motes are randomly placed, and its pdf is f_{PDIF}. From (9)–(14), the location estimation errors from different physical error sources including the random and systematic errors can be quantified. Intuitively, the error sources that vary $P_{r,1}$ and $P_{r,2}$ most will degrade the performance most seriously. Therefore, the major phenomenon that cause location estimation errors would be the fading effect which fluctuates received signal strengths as far as 10 dB and cannot be effectively mitigated by increasing the signal to noise ratio. The numerical and simulation results will be further compared in Section III-E.

III. Ability of a Single Mote to Do Location Detection by Itself in Absence of Neighbors

A. Testbed Setup

Crossbow MICA2 motes, used as examples of simple wireless sensor nodes for our testbed, have the capability to sense light, temperature, humidity, sound, two-axis acceleration, and a two-axis magnetic field. Quarter wave whip antennas are used on the target motes which are standard compact omnidirectional antennas that come with the sensor mote. Semi-directional patch antennas are chosen to be deployed on the anchor motes because of their simple fabrication, small size, and low cost. The anchor motes are used to receive and the target motes to transmit. The solution of the location determination equations is done at the receiver. The patch antennas are slightly more complex than the whip antennas in fabrication, but can provide semi-directional radiation pattern that covers approximately 90 degrees (3 dB beamwidth of this patch antenna is 121 degrees). These were fabricated in house using a milling machine, a relatively low cost fabrication equipment. The transmitted power is set at 0 dBm which can be increased according to the required SNR concerning the system performance and the power consumption. The overall system loss factor is measured to be -10.32 (dB) in anechoic chamber including motes output power offset (-5.3), efficiency of transmitting and receiving antennas (-1.43), impedance mismatch (-1.64), insertion loss of switch (-0.55), and cable loss (-1.4).

The choice of the directional antenna for transmitting is controlled using a switching network, implemented with a Hittite GaAs MMIC SP4T switch. The cost of the switch is $2.43, representing a marginal increase in total cost to the circuitry. The switching time from one antenna to the next is 150 ns, a rate considered acceptable for the low bit rate sensor motes communication in our experiments, so the switching mechanism will not affect the data transmission. The insertion loss is 0.55 dB at 916 MHz. Therefore, this switching mechanism increases the hardware and software cost only slightly while not significantly sacrificing range and receiver sensitivity. Also the testbed is designed to have the capacity of simultaneously collecting the signal strength received by the omnidirectional antennas which provides a good tool to benchmark with the traditional localization schemes.

B. Performance Metric

The performance is measured by the location error which is defined by the error distance from the estimated target position

$\rightharpoonup \hat{r}_{\text{target}}$ to the actual target position $\rightharpoonup \hat{r}_{\text{target},0}$ divided by the known actual distance between the anchor mote and the target mote ($R = |\rightharpoonup \hat{r}_{\text{anchor},0} - \rightharpoonup \hat{r}_{\text{target},0}|$) where $\rightharpoonup r$ is a position vector. Location error in percent is as defined follows:

$$R_{\text{error,relative}} = \frac{|\rightharpoonup \hat{r}_{\text{target}} - \rightharpoonup \hat{r}_{\text{target},0}|}{|\rightharpoonup \hat{R}|} = \frac{|\rightharpoonup \hat{r}_{\text{target}} - \rightharpoonup \hat{r}_{\text{target},0}|}{|\rightharpoonup \hat{r}_{\text{anchor},0} - \rightharpoonup \hat{r}_{\text{target},0}|}. \quad (15)$$

In case of multiple anchor motes, we use the absolute error instead of relative error because there are cases that target motes are very close to one of the anchor motes and far away from the others and the average percent error is less meaningful in such situations

$$R_{\text{error,abs}} = |\rightharpoonup \hat{r}_{\text{target}} - \rightharpoonup \hat{r}_{\text{target},0}|. \quad (16)$$

C. Effects of Truncations and Approximation for Simple Implementation on Modes

We use a polynomial Taylor series expansion to approximate $\hat{\Theta}$ and $\hat{r}$ from (3) and (4). With this approximation, only a few coefficients need to be stored in the motes, which greatly reduces the memory storage requirements on the motes. For example, a polynomial of order four is feasible for the limitation of both storage and computation on motes, and (3) (the equation for the determining angle estimates) can be expended in Taylor series and stored with five coefficients, (in our testbed example for the patch antenna, 1.0262×10^{-5}, $-14837\times10^{-5}, -1.6036\times10^{-5}, -5.5999, 45.077$). Furthermore, this approximation reduces the processing time for location computation.

To compare the error resulting from the numerical approximation and truncation, the location estimation is computed from the random test positions, and those estimates are solved by two methods (least squares numerical method and approximated polynomial equations) in three cases. The first is the least squares numerical method which considers the small Θ_c. The second and the third cases are polynomial approximations of order ten and order four which both neglect Θ_c. The order of the polynomial is critical on motes due to their limited computational power and limited memory (4 MHz and 128 KB for a MICA2 mote). The results of the polynomial approximations are shown in Fig. 4. The result shows that the errors caused by neglecting Θ_c and the polynomial approximation are very small. The approximate solution of (3) matches the precise solution computed using MATLAB with an average absolute location error of 9.3 cm when the order of the polynomial is ten. When the approximation is truncated to an order of four, the average absolute location estimation error grows to 0.628 meters. The mean location estimation error increases from 30.42% (order of ten) to 32.07% (order of four). The error increases due to the approximation of the radiation pattern and the inverse function. Therefore, there is tradeoff between the truncation order (storage memory and running time) and the accuracy; the more precise information of antenna patterns, the more accurate location estimation could be.

The comparison between these approximations is shown in Table I. The truncation and approximation makes the proposed algorithm able to be implemented, fast, and with low storage memory requirements with a slight increase of location estimation error. Concerning the running time, our proposed scheme consumes a low computation power within less than 500 ms; meanwhile, only two RSSIs are taken in a single mote in addition to switching power consumption (about 100 μW), whereas using triangulation needs to operate three motes, so our proposed scheme is more energy efficient for the network as a whole.

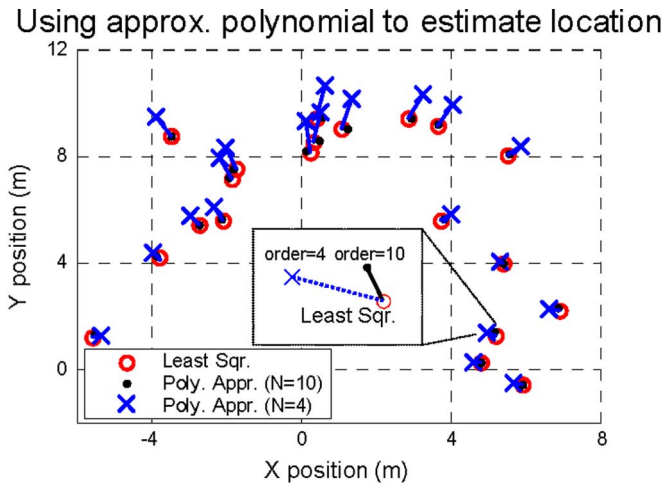

Fig. 4. Location estimation error with polynomial approximation; the circle marks are the setup positions.

TABLE I
COMPARISON WITH APPROXIMATIONS

Numerical algorithms	Complexity	PC running time (ms)	Requirement for storage memory
MATLAB	High, run on PC	1964	Algorithm to solve non-linear eqn
Polynomial order = 10	Low, run on motes	410	Polynomial ftn with 11 coeff's
Polynomial order = 4	Low, run on motes	406	Polynomial ftn with 5 coeff's

D. Analytically Estimated r and θ in the Presence of a Faded Channel

A target is assigned to an arbitrary position, say $R_0 = 7.32$ meter and $\Theta_0 = 30$ degrees, and we assume that the distributions of the received strength through channels from patch antenna #1 and patch antenna #2 are independent Rician distributions. Through a separate set of experiments received signal strengths from semi-directional antennas oriented different directions are collected and correlation coefficients are calculated. The correlation between the received signal strengths on two directional antennas is low in our measurements. Thus we can justifiably make the assumption of independence of $P_{r,1}$ and $P_{r,2}$ as made in (9). The parameters $K(K_i = A_i^2/\sigma_0^2, i = 1, 2)$ of the Rician distributions are empirically obtained by fitting the statistics of the measured received signal strength, and let $K_1 = K_2$, assuming that in the same environment the statistical property is similar though the actually multipaths are not the same from point to point. Let $A_i\sqrt{(P_{r,i,\text{no fading}})}, i = 1, 2$ where

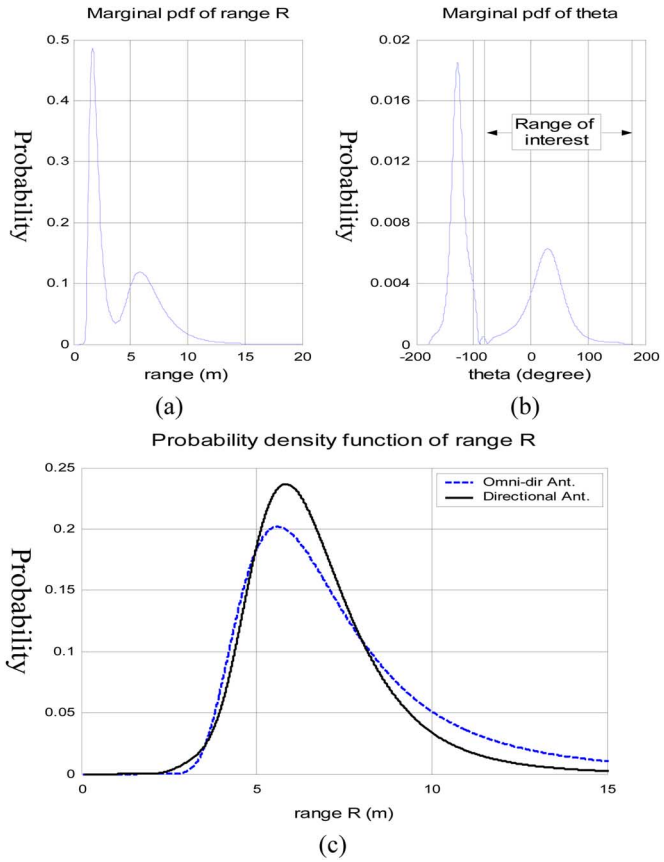

Fig. 5. (a) Marginal distribution of range estimation R; (b) the angular marginal distribution; (c) marginal pdf of R of patch antenna (solid line) and monopole antenna (dashed line) on the restriction Θ region.

$P_{r,i,\text{no fading}}$ is obtained at the specific position according to Friis' formula. In our testbed, the nodes with the patch antennas also have a monopole omnidirectional antenna. Thus, the data from the directional system and the omnidirectional system can be obtained at the same time. This results in a valid comparison between the accuracies of the two systems.

The joint distribution is numerically calculated according to (9). The marginal pdfs of range R and Θ are derived from the joint distribution through integration and shown in Fig. 5(a) and (b). These marginal pdfs provide the estimated R and Θ varying correspondingly with the uncertainties of the received strengths under the fading channel by using maximal likelihood estimation except that there are two possible regions since the solutions of this system are not unique. Only one is a feasible solution and the other one is infeasible due to the nature of the directional antennas in use as discussed in Section II-B. In this example, there are two peaks occurring, one is at $\Theta = 30.0$ degree, range $R = 5.85$ m, and the other is at $\Theta = -128.5, R = 1.65$ m. The feasible solution of the estimation is $R = 5.85$ meter, and $\Theta = 30.0$ degrees. The second solution is infeasible and discarded. Any solution where Θ is out of the applicable domain $[-79, 160]$ [see Fig. 5(b)] is infeasible because the signals of directional antennas are only used in front of them. A straightforward way to determine this applicable domain of Θ is observed from the range of $G'_{\text{diff}}()$ in (7.a). The infeasible solution is removed from the marginal pdfs and they are normalized (to sum to 1). This transformed distribution for R is shown in Fig. 5(c).

TABLE II
LOCATION ERROR CAUSED BY DIFFERENT PHYSICAL PHENONENON

	Noise SNR= 12dB	RSSI ±2.343 dB	Rician K= 4.925(dB)
STD of Θ (degrees)	2.274	7.231	28.884
STD of R (m) (% = STD of R / R_0)	0.114 (1.6%)	0.428 (5.8%)	2.628 (35.9%)

It is interesting to compare the data sets for the directional antennas with those collected for the omnidirectional antennas. In order to make a comparison, we do the analysis for the omnidirectional antennas to find the distribution of the pdf of R_{omni}. These results are compared with the marginal pdf R_{dir} of the directional antenna which is obtained by using $R_{\text{omni}} = \text{constant}/\sqrt{P_r}$ [see Fig. 5(c)], and the estimated $\hat{r}$ from these two pdfs are denoted, $\hat{r}_{\text{omni}}$ and $\hat{r}_{\text{dir}}$. We found that the standard derivation of R_{dir} (2.6279) is smaller than that of R_{omni} (4.3275) and meanwhile the estimated $\hat{r}_{\text{dir}}$ using directional antenna (5.850) is closer to the setting R_0 than the estimated $\hat{r}_{\text{omni}}$ using omnidirectional antenna (5.613). That means the estimation of R for directional antennas is more reliable than that of the omnidirectional antenna under the same environment, and also implies that the communication channel should also be more reliable using the directional antennas. This is because the directional antennas have one more constraining factor, angular information, which improves the location determination.

E. Analysis of Location Estimation Errors

The location estimation errors comes from several factors: a) noise from channel or from the whole system; b) accuracy of the RSSI; and c) channel models for path-loss equation as well as received strength variation caused by channel impairment such as multipath fading effects. In this section, the effects of these random factors on the performance of the location estimation error are compared based on the theoretical analysis presented and detailed in Sections II-B and II-C. The location errors are evaluated by analytic or numerical methods and verified with simulations that the target mote is set at ($R = 7.32$ m, $\Theta = 30$ degrees). A comparison of the error sources is shown in Table II and detailed in the following subsections.

Additive noise—The description of the analysis of additive noise is detailed in Section II–C. The two strongest received strengths at the set position are -52.56 dBm and -55.16 dBm when $\text{transmitting power} = 0$ dBm. The noise floor is assumed to be -70 dBm as a lower bound for practical wireless receivers. In practice, the noise floor of the mote is lower than -80 dBm. The SNR is set to be 12 dB as a worst case. The variance of Θ and R are calculated by (12) and (B.1), and the numerical results show that the standard deviations of the Θ and R are 1.981 (degrees) and 0.1153 (m), respectively, which are close to the simulation results as Table II.

RSSI errors—A part of the estimation errors result from RSSI errors due to inaccuracy of the low-cost, simple RSSI on the mote. To quantify this RSSI error, the power strength between the RSSI and the spectrum analyzer are compared by feeding sweeping power levels of the same transmitting source through direct cable connections. Errors as a function of RSSI are not

linear but bounded. The maximum difference is about 2.343 dB over our measurement range (-45– $-$ 85 dBm). Using (14) which evaluates angular variance caused by inaccuracy of RSSI, the upper bound of standard variation of Θ is calculated to be 10.96. The simulation results show the standard deviations of the Θ and R are 7.231 (degrees) and 0.428 (m), respectively.

Channel fading—Significant research has been done to investigate more practical and accurate channel propagation models [13], [19] and parameter estimations [20], so in this paper, we do not emphasize on fitting the channel models and the parameters. We provide a generic approach to analyze the effects of those random and systematic factors including noise, measurement errors, and fading channel on the performance of location estimation. We use the most basic propagation equation as a coarse estimate to prove that our approach works, since an exact description of propagation is most often not possible in a realistic setting. This represents worst case scenario and demonstrates that this approach still works under this assumption. While utilizing more refined channel models, the same approach can be applicable to determine the location more accurately and again estimate the location error range.

The channel variation under Rician fading is considered. The analysis is shown and discussed in the previous section, and the standard deviations of the Θ and R are 28.884 (degrees) and 2.628 (m). The K factor is estimated to be 4.925 (dB) from the statistics of the received strengths in a realistic outdoor environment. Therefore, we can observe that the major error sources is due to the erroneous fading channel caused by multipath effect, which might cause received signal strength drops as far as 10 dB down. The comparison of the different mechanisms can be summarized in Table II. This error analysis shows the channel is the dominant consideration and that turning the transmission power up or using more accurate receiver components have marginal effects.

F. Effect of Design Choices: Radiation Pattern and Signal to Noise Ratio on a Single Simulation

In addition to the impact of the stochastic channel on the estimate of R and Θ, another important factor is the directivity of the antenna. Since angular variation in the radiation pattern is being used in the calculation of the location, it is important to understand the effect of the angular spread of the pattern on the location determination. While obviously a very directional antenna could be used to pinpoint the angle of arrival of a signal, the large size of these antennas makes them infeasible to realize on compact wireless devices. Therefore semi-directional radiators such as patch antennas are utilized, but an investigation on the effect of the directionality is warranted. Instead of fabricating a large number of antennas of different directivities, simulations are executed to investigate the influence of the directivity under the AWGN channel and fading channel. In order to quantify effect of antenna beamwidth and separate the effects of antenna gain or SNR, we define a term called *directivity order*, denoted as N. The directivity order of the measured radiation pattern $G_t(\Theta)$ is taken as the reference $(N = 1)$. A higher directivity order indicates a narrower beam. In practice, this would also increase the maximum gain. However, in order to study the effect of the beamwidth in isolation, we normalize and keep

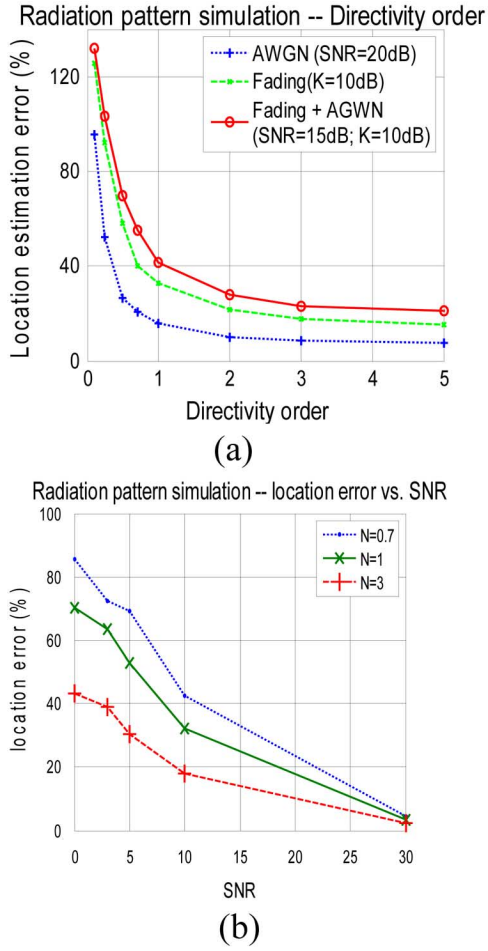

Fig. 6. Location estimation versus (a) directivity order; (b) increased SNR.

maximum gain constant at the same value as for $N = 1$, namely, $G_{\max}$. The modified radiation pattern is denoted $G_{\text{test}}(\Theta, N)$

$$G_{\text{test}}(\Theta, N) = G_{\max}\left(G_t(\Theta)/G_{\max}\right)^N. \tag{17}$$

As the order N increases, the antenna beamwidth becomes narrower; while at $N \rightarrow 0$, it becomes the omnidirectional antenna. A higher dielectric constant in the patch will allow a smaller form factor, but decrease the pattern directivity. This simulation helps to determine an acceptable range of the directivity order. The simulation results are shown in Fig. 6. The performance of location estimation using our designed patch antennas can be observed at $N = 1$ with suitable environmental parameters (noise floor, fading rate, and SNR).

We found that as directivity order N increases, the location estimation performance improves; however, this improvement is not significant beyond $N = 3$ in the simulation. The breaking point is close to $N = 1$, which describes semi-directional antennas with gain $\sim$6 dBi and covers a typical beamwidth of 60–120 degrees. Therefore, semi-directional antennas (such as a simple patch antenna) are deemed the suitable choice for location determination under the tradeoff between cost and acceptable performance, particularly on small scale wireless nodes. The results also show the effect of increasing SNR on the location estimation accuracy. A higher SNR may be caused by

increase in transmission power or by higher antenna gain. Expectedly, the location estimation accuracy increases with higher SNR, and the amount for different types of patterns is quantified in Fig. 6.

IV. Effect of Multiple Anchors on the Accuracy of Location Determination

In theory, the performance of location estimation with multiple anchor motes should be better because of the reliance on location information from other motes. However, the quantitative improvement would depend on the relative placements of the anchor motes. Since it is infeasible to do exhaustive experiments on extremely large networks, simulations are performed in MATLAB for a wide number of network scenarios and topologies. Target motes are evenly spread into a square area, called the *testing region*. Various network topologies are assigned to four anchor motes receiving four-oriented signal power strengths which are processed through the effects of pathloss, white Gaussian noise, Rician fading channel, and the directional antenna. Equations (7) and (8) are used to obtain the individual estimates from each anchor mote, and the location is aggregated by averaging over all the estimates by (5). The significant result from the simulations is that the performance of our proposed scheme is less sensitive to the relative placement of the anchor motes than triangulation based schemes, which is further verified by measurements in following sections. Specifically in Section V, outdoor experiments of multiple anchor motes in a network are performed to verify that the anticipated simulated performance is possible even with poor network topologies such as linear arrangements of motes and/or anchor motes placed closely.

A. Multiple Anchor Simulation—Estimating Performance According to Different Topologies

The goal of the experiments is to compare the location estimation accuracy between the independent estimates using directional antennas (proposed scheme) and triangulation using omnidirectional antennas (traditional scheme). Twelve topologies of four anchor motes are arranged separately in squares of 4.88×4.88 meter^2 grid (Area A, small), 12.2×12.2 meter^2 grid (Area B, medium), and 24.4×24.4 meter^2 grid (Area C, large). The transmitted power is -10 dBm. The envelope of received signal strength through the wireless channel is simulated using a Rician fading channel (parameter K factor $= 10$ dB) with noise floor $= -70$ dBm. Each estimate error from different topologies is based on the average of 1000 different samples of target motes evenly distributed in the square of test region. For each topology, the anchor motes are placed according to Fig. 7.

The desirable performance point is that the performance of the location estimation scheme should be relatively insensitive to which topology is used. This makes the deployment of the network feasible for large numbers of nodes.

Representative results of location estimation of topologies #8 and #12 in Area B using proposed and traditional schemes are shown in Figs. 8 and 9. The topology #8 represents the anchor motes placed at the edge of the testing region and located

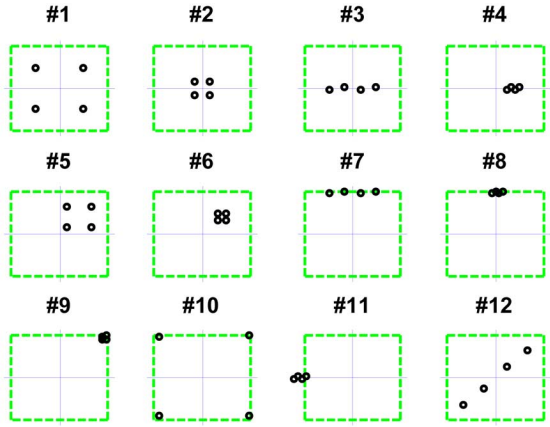

Fig. 7. Twelve different topologies #1–#12 of anchor motes setup (unit is meters). Target motes are evenly distributed in the square area, so-called testing region, shown by the dashed square of 20×20 square feet.

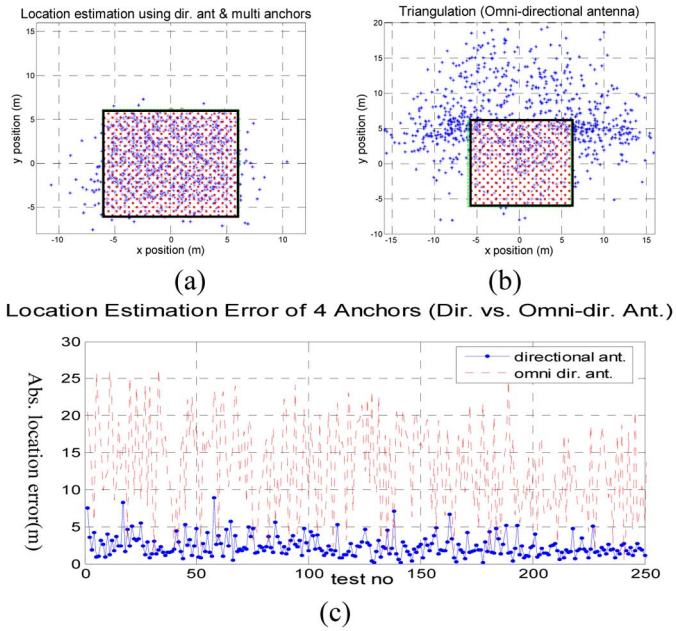

Fig. 8. Location estimation result of topology #8.

close to each other, and the topology #12 represents the anchor motes distributed on the testing region but in a linear placement. The estimation from independent location determination shows more accurate estimation than the triangulation. The average errors are respectively 1.488 and 7.675 meters in topology #8 and 1.167 m and 3.756 m in topology #12. In Fig. 8(a), 91.53% of the estimated positions of target motes are within the testing region and have the location error less than 4 meters, but in Fig. 8(b) which is the result of location estimation using triangulation, 64.17% estimated target positions are out of this testing region, and have larger location estimation error than our proposed scheme [Fig. 8(c)]. For topology #12, 93.09% and 84.95% are within the testing region using our proposed scheme and triangulation, respectively. When the placement of anchor motes is linear [Fig. 9(b)], i.e., the anchor motes are laid co-lined, the ambiguity of determining the positions on the right side occurs

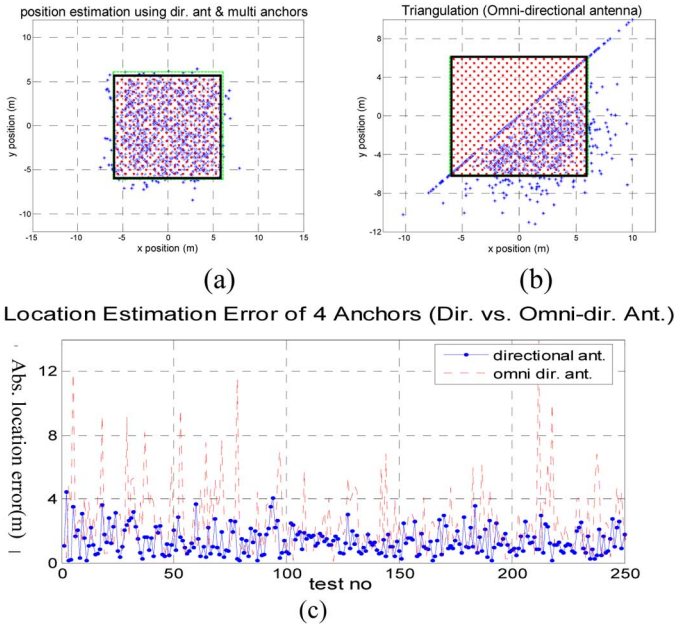

Fig. 9. Location estimation result of topology #12.

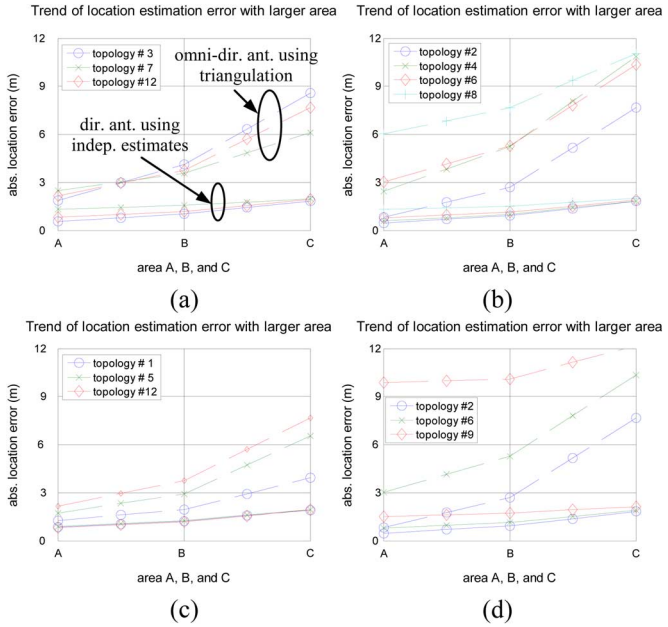

Fig. 10. Trend of location estimation error of Area A, B, and C in type (a) linear; (b) small separated; (c) evenly distributed; (d) centralized. The solid and dashed lines represent the proposed algorithm and the triangulation.

TABLE III
PERFORMANCE OF BEST AND WORST CASE SCENARIOS

	Area A (m x m) 4.88 x 4.88		Area B (m x m) 12.20 x 12.20		Area C (m x m) 24.40 x 24.40	
	Directional antennas	Omni antennas	Directional antennas	Omni antennas	Directional antennas	Omni antennas
Mean	0.9950	3.3115	1.3048	4.8081	1.9360	8.2346
STD	0.3826	2.6336	0.2750	2.4992	0.0906	2.8820
Worst	1.4993(#9)	9.8949(#9)	1.7324(#9)	10.0959(#9)	2.1240(#9)	12.1990(#9)
Best	0.4701(#2)	0.8249(#2)	0.9216(#2)	1.9483(#1)	1.8150(#2)	3.3018(#10)
Ratio	3.1893	11.9953	1.8798	5.1819	1.1702	3.695

Mean and STD: the average and the standard deviation of the twelve scenarios; worst and best indicate the worst and best performance of location estimation error, which occur in (topology no); Ratio: the ratio of worst case over best case.

in triangulation method and not in our scheme, because the triangulation does not work well in this condition and additional information is required.

While two sample data sets are presented in detail in the figures above, it is instructive to see how the methodologies compare in general. The average location estimation errors of these twelve topologies by independent estimates using directional antennas are 0.9950, 1.3048, and 1.9360 (meters) in Area A, B, and C, respectively, and the errors using triangulation with omnidirectional antennas are 3.3115, 4.8081, and 8.2346, respectively (see Table III).

From these simulation results, we posit that there are three main factors in the topology that significantly affect the performance of triangulation based schemes, but are not deleterious to our proposed scheme.

a) *Linear placement*: When anchor motes line up (topology #3, #7, #12), triangulation is ill-conditioned (no triangle is formed among these anchor motes), and at the same time, it encounters ambiguity in determining the side on which the target mote is located.
b) *Separation distance between anchors*: As the separation distance between anchors decreases, the location estimation error increases—compare the relative performances in topology #1& #2, #3 & #4, #5 & #6, and #7 & #8.
c) *Distributed evenly*: Laying down the anchor motes around the four different corners, evenly spread out, improves the location estimation performance (topology #1, #12, and #5).

From Table III, we see that the ratio of the worst case error to the best case error of our scheme is about one-third of the traditional method, and the variances are smaller for all three field sizes in our approach. In summary, while using triangulation with omnidirectional antennas, the planning of the topology of anchor motes is critical while our proposed scheme with directional antennas is far less relevant to the placement. Furthermore, in Area B and Area C, the worst performance of our proposed scheme is still better than the best case of the traditional scheme among these topologies.

B. Multiple Anchor Simulation—Estimation Location Error With Increasing the Area

A comparison of the scalability of the two approaches is of interest as well, since the performance claims are meant to be broadly applicable. We observe from Table III that as the area increases (A to B to C), the location estimation error increases. For this set of experiments, we consider four different classes of topologies—linear (topologies #3, #7, and #12), small separated (topologies #2, #4, #6, and #8), evenly distributed (topologies #1, #5, and #12), and centralized (topologies #2, #6, and #9). The location estimation errors for the three field sizes are shown in Fig. 10. The rate of increase in the error is always greater for the triangulation approach compared to our approach, except for topology #9 in which the performance of triangulation is already at its worst. From these results, we conclude that our proposed scheme is relatively insensitive to the size of the area.

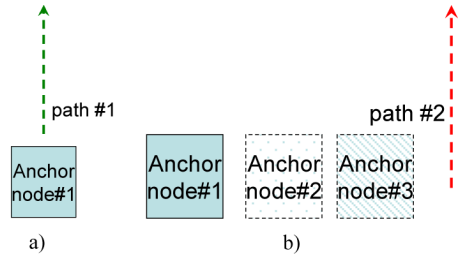

Fig. 11. Separated single motes are laid along path #1 and #2 on outdoor area of 40 × 40 feet 2. (a) (path #1) a straight path perpendicular to the nearest antenna face with one anchor #1 and (b) (path #2) a straight path parallel to the nearest antenna face with three anchor motes #1–#3.

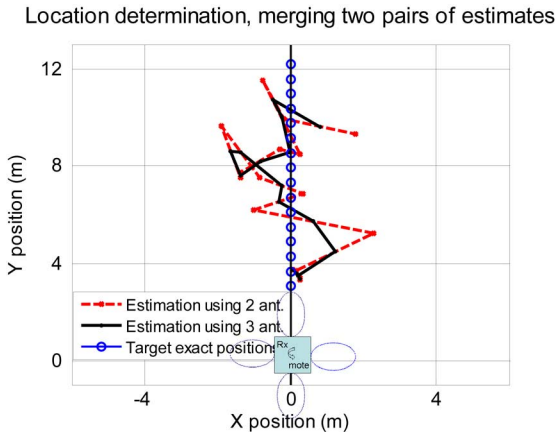

Fig. 12. Single mote location determination of path #1. The dashed lines are the initial location estimation. The solid lines are the location estimation result merging estimates from three antennas.

V. Experimental Results and Discussions

Anchor motes equipped with the four directional antennas monitor the RSSIs for each separate antenna and select the two strongest to compute the location of the target motes. The motes are tested in a typical outdoor environment which is a broad street between the buildings on campus to observe the performance of the location determination system in a practical wireless channel. The goal of the experiments is to determine the estimation error of the location determination system in wireless sensor networks with both single and multiple anchor motes. Path #1 which is supposed to have constant angle estimation is set up to demonstrate the procedure, and path #2 is to test the performance of the multiple anchor motes and compare with omnidirectional antennas using triangulation (as Fig. 11).

A. Independent Location Estimation—Single Anchor

The location estimation by a single anchor is tested with respect to the location error. The target motes are placed in meters from position (0, 3.05) to (0, 12.19) on path #1. The estimation is computed by selecting the two patch antennas with the strongest RSSIs using (7) and (8). The location estimation error of path #1 is 32.10% (2.46 meters) on average. The result of using a single mote to estimate the target mote on path #1 is shown with dashed line in Fig. 12. The location estimation error can be furthermore reduced by further processing the location

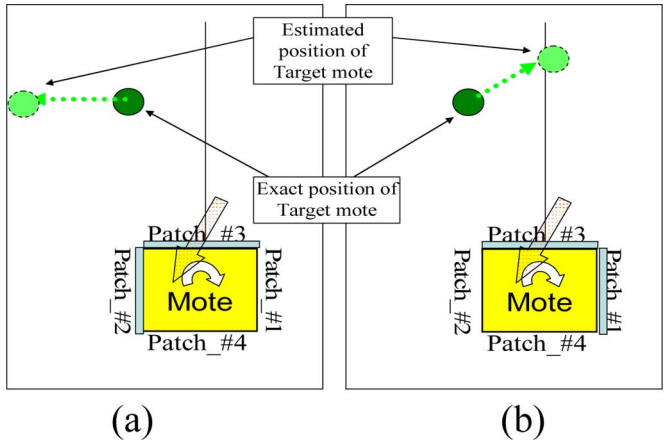

Fig. 13. Location estimation with merging estimates from three antennas. Single estimate (a) from antenna set, #2 & #3; (b) from antenna set, #1 & #3.

estimates with the additional estimates from the other antenna as below [6].

With merging estimates from three antennas—In this method, instead of two patch antennas, three are used at the same time when the second and third smaller RSSIs have little difference. For the case of the difference is less than 3 dB, the angle of target motes might be from $(-15, 15)$ degrees with respect to the orientation of closest directional antenna. Two location estimates are made in one anchor mote by using three adjacent antennas at the same time, the final result is obtained by averaging these two estimated locations. The location error decreases from 32.10% (by using two antennas #1 and #3) to 19.55% (by using three antennas #1-3). The result is shown in Fig. 12. Fig. 13 shows the illustration of physical phenomenon explaining the compensation by using different orientations of antennas pairs on the same motes. When the received signal of antenna #3 happens to drop, the estimated angle by the antenna set, #2 and #3, is over-estimated [Fig. 13(a)]. For the other antenna set, #1 and #3, the estimated angle is under-estimated [Fig. 13(b)]. Therefore, the location error can be compensated from multiple antenna pairs of estimates.

B. Topology Insensitivity Performance—Multiple Anchors

Two more anchor motes are added to assist location determination for path #2. To demonstrate the contrast with triangulation, a scenario that would give poor accuracy in triangulation is chosen, namely, a linear topology of the anchor motes. The target collects the position estimates from each of the three anchor motes and averages these three by (5). The results are shown in Fig. 14. The location estimation error is 13.17% Furthermore, using multiple anchors for location estimation not only results in good estimation, but also makes this system more robust in case that some anchor motes or wireless links lose their connectivity.

During the previous experiment, measurements are also made using omnidirectional antennas on the anchor motes. The testbed is equipped with the directional patches, as well as a monopole to compare directly to more traditional means of location detection. The received strength at the omnidirectional antennas are recorded and used to estimate the ranges between

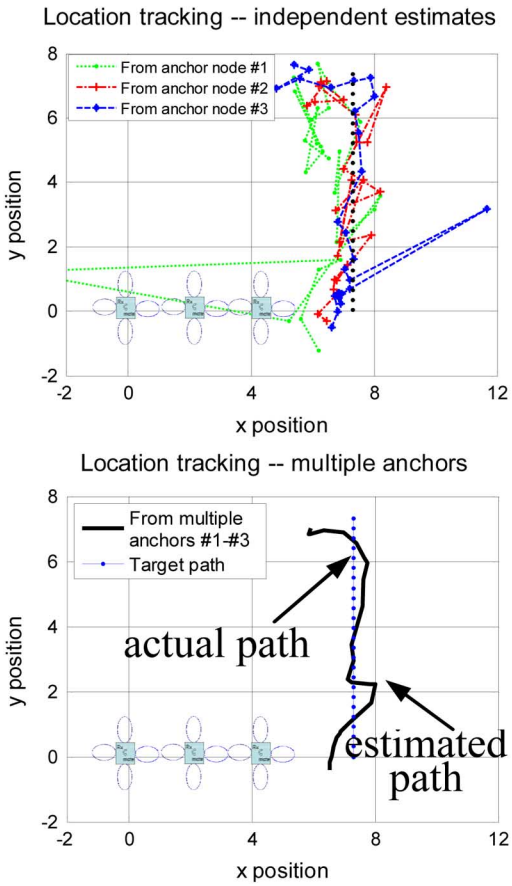

Fig. 14. Outdoor location determination with multiple anchor motes of path #2. (a) independent estimates; (b) synthesized from multiple anchor motes.

the target motes and the anchor motes. Then, the least-squares approach is applied to find the best-fit estimated location (x, y) for the equation set

$$(\hat{x} - x_i)^2 + (\hat{y} - y_i)^2 = d_i^2 \tag{18}$$

where (x_i, y_i)'s are the positions of the anchor motes.

After some manipulation, this equation set can be rewritten in a linear matrix form [16]

$$2\begin{bmatrix} x_n - x_1 & y_n - y_1 \\ \vdots & \vdots \\ x_n - x_{n-1} & y_n - y_{n-1} \end{bmatrix}\begin{bmatrix} \hat{x} \\ \hat{y} \end{bmatrix} = \begin{bmatrix} (d_1^2 - d_n^2) - (x_1^2 - x_n^2) - (y_1^2 - y_n^2) \\ \vdots \\ (d_1^2 - d_n^2) - (x_1^2 - x_n^2) - (y_1^2 - y_n^2) \end{bmatrix}. \tag{19}$$

(19) is represented as $\mathbf{Ax} = \mathbf{b}$; and the solution, $\mathbf{x} = (\hat{x}, \hat{y})$, of minimizing $||\mathbf{Ax} - \mathbf{b}||_2$ is $\mathbf{x} = (\mathbf{A}^T\mathbf{A})^{-1}\mathbf{A}^T\mathbf{b}$; $(\mathbf{A}^T\mathbf{A})^{-1}$ is the pseudo inverse of matrix $\mathbf{A}^T\mathbf{A}$.

The location error of triangulation using an omnidirectional antenna is 49.84% which is four times the location estimation error of our proposed algorithm using directional antennas. The paths traced by omnidirectional and directional antennas are as shown in Fig. 15, with the proposed scheme nearly looking indistinguishable from the actual path relative to the triangulation results. The actual path #2 does not cause the target mote's x-coordinate to change and this is estimated with directional antennas well.

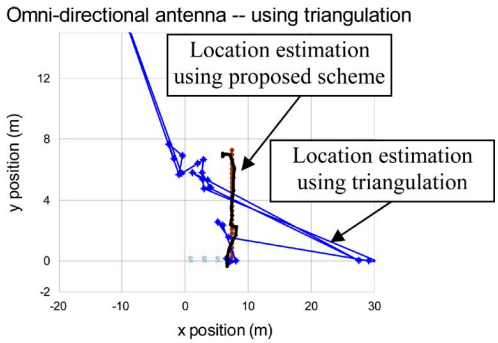

Fig. 15. Comparison of triangulation and our proposed scheme for path #2.

VI. Conclusion

In this paper, a location determination algorithm using a single anchor to create an individual estimate has been proposed for sensor networks and verified in a physical testbed consisting of Crossbow motes. A single mote was enabled to estimate location with a 30% error on average by adding a simple switch and four directional patch antennas. This result, while potentially useful in its own right, was demonstrated to be beneficial when extended to multiple anchor motes to provide more accurate location estimation. The performance of location estimation error was shown by simulation and by experiments to be insensitive to the network topology of anchor motes. The computational complexity of the proposed scheme is similar to the algorithm for location estimation using a single anchor. In our testbed, this decentralized algorithm is shown to need low memory storage requirements, low latency of execution, and low energy consumption, all suitable for the most inexpensive of sensor boards.

Factors affecting the performance of location determination such as the fading channel, RSSI errors, noise, and the antenna radiation pattern were investigated through simulation. By using this technique to estimate location of target motes, the location estimation errors are mitigated by one-third compared to triangulation with omnidirectional antennas. Furthermore, considering different topologies of anchor motes, the location estimation error of our proposed scheme ranges from 0.92 (m) to 1.73 (m) (ratio $= 188\%$) while using triangulation the location estimation error ranges from 1.95 (m) to 10.10 (m) (ratio $= 518\%$), and this shows our simple location estimation algorithm is relatively insensitive to the topology and slow growth of error with large area. Thus, we have shown that a relatively unsophisticated and inexpensive hardware modification to the sensor mote allows a single mote to detect a significant amount of location information, and the multiple anchor motes provide a more robust and flexible topology system with smaller location estimation error.

Appendix

A. Single Anchor—Manipulation of the Optimal Location Estimation Formula

The randomness of the wireless channel is taken into account, so (2) is expressed to (6) in dB to find the range and angle esti-

$$
\begin{aligned}
&\operatorname{var}(\hat{r} \mid P_{r,2} > P_{r,1}) \\
&\quad = \operatorname{var}\left(\left(\frac{P_t^2 G_t G_r(\hat{\Theta}_1) G_t G_r(\hat{\Theta}_2)}{P'_{r,1} P'_{r,2}} \right)^{1/4} \right) \\
&\quad \approx \operatorname{var}\left(\left(\frac{P_t^2 G_t^2 G_r \left(\sum_{i=1}^{\tilde{N}} c_i \left(\frac{P_{r,1}+n_1^2}{P_{r,2}} \right)^i \right) G_r \left(\left[\sum_{j=1}^{\tilde{N}} c_j \left(\frac{P_{r,1}+n_1^2}{P_{r,2}} \right)^j \right] - \frac{\pi}{2} \right)}{(P_{r,1}+n_1^2)(P_{r,2})} \right)^{1/4} \right) \\
&= \operatorname{var}\left(\left(\frac{P_t^2 G_t^2 G_r \left(\sum_{i=1}^{\tilde{N}} c_i n'^i_1 \right) G_r \left(\left(\sum_{i=1}^{\tilde{N}} c_i n'^i_1 \right) - (\pi/2) \right)}{n'^i_1 P_{r,2}^2} \right)^{1/4} \right) \\
&= \int_{-\infty}^{\infty} \left(\frac{P_t^2 G_t^2 G_r \left(\sum_{i=1}^{\tilde{N}} c_i n'^i_1 \right) G_r \left(\left(\sum_{i=1}^{\tilde{N}} c_i n'^i_1 \right) - (\pi/2) \right)}{n'^i_1 P_{r,2}^2} \right)^{\frac{1}{2}} \times \frac{e^{-\frac{n_1^2}{2\sigma^2}}}{\sqrt{2\pi}\sigma} dn_1 \\
&\quad - \left(\int_{-\infty}^{\infty} \left(\frac{P_t^2 G_t^2 G_r \left(\sum_{i=1}^{\tilde{N}} c_i n'^i_1 \right) G_r \left(\left(\sum_{i=1}^{\tilde{N}} c_i n'^i_1 \right) - (\pi/2) \right)}{n'^i_1 P_{r,2}^2} \right)^{\frac{1}{4}} \times \frac{e^{-\frac{n_1^2}{2\sigma^2}}}{\sqrt{2\pi}\sigma} dn_1 \right)^2
\end{aligned} \tag{B.1}
$$

mation using optimization theory. Equation (6) can be re-written as (A.1)

$$
\begin{aligned}
&f_{\text{error}}(r, \Theta_1, \Theta_2) \\
&\quad = (P_{t,\text{dB}} + G_{t,\text{dB}} + G_{r,\text{dB}}(\Theta_1) \\
&\qquad - 2\log(r) - P_{r1,\text{dB}})^2 \\
&\qquad + (P_{t,\text{dB}} + G_{t,\text{dB}} + G_{r,\text{dB}}(\Theta_2) \\
&\qquad - 2\log(r) - P_{r2,\text{dB}})^2; \\
&\quad = (K_1 + G_{r,\text{dB}}(\Theta_1) - 2\log(r) - P_{r1,\text{dB}})^2 \\
&\qquad + (K_2 + G_{r,\text{dB}}(\Theta_2) - 2\log(r) - P_{r2,\text{dB}})^2; \\
&\min_{\Theta_1,\Theta_2,r}\{f_{\text{error}}(r, \Theta_1, \Theta_2)\}, \\
&\qquad\qquad \text{s.t.} \hat{\Theta}_2 = \hat{\Theta}_1 - \tfrac{\pi}{2} - \tfrac{d}{\hat{r}}.
\end{aligned} \tag{A.1}
$$

According to optimization theory, the minimal solution occurs at $\partial f_{\text{error}}/\partial r = 0, \partial f_{\text{error}}/\partial \Theta = 0$

$$
\begin{aligned}
&\frac{\partial}{\partial r} f_{\text{error}}(r, \Theta_1, \Theta_2) \\
&\quad = 2\left(K_1 + G_{r,\text{dB}}(\Theta_1) - 2\log(r) - P_{r1,\text{dB}}\right)\left(\frac{-2}{r}\right) \\
&\qquad + 2\left(K_2 + G_{r,\text{dB}}(\Theta_2) - 2\log(r) - P_{r2,\text{dB}}\right) \\
&\qquad \times \left(G'_{r,\text{dB}}(\Theta_2)\left(-\frac{d}{r^2}\right) - \frac{2}{r} \right) = 0.
\end{aligned} \tag{A.2}
$$

The $G'_{r,\text{dB}}$ is finite in the range $[0, 2\pi)$, and d/r^2 is very small, so we neglect terms to simply the derivations

$$
\begin{aligned}
&\frac{\partial}{\partial \theta} f_{\text{error}}(r, \Theta_1, \Theta_2) \\
&\quad = 2(K_1 + G_{r,\text{dB}}(\Theta_1) \\
&\qquad - 2\log(r) - P_{r1,\text{dB}})(G'_{r,\text{dB}}(\Theta_1)) \\
&\qquad + 2(K_2 + G_{r,\text{dB}}(\Theta_2) \\
&\qquad - 2\log(r) - P_{r2,\text{dB}})(G'_{r,\text{dB}}(\Theta_2)) = 0
\end{aligned} \tag{A.3}
$$

(A.2) and (A.3) can be further manipulated as follows:

$$
\begin{aligned}
&K_1 + G_{r,\text{dB}}(\Theta_1) - 2\log(r) - P_{r1,\text{dB}} \\
&\qquad + K_2 + G_{r,\text{dB}}(\Theta_2) - 2\log(r) - P_{r2,\text{dB}} = 0
\end{aligned} \tag{A.4}
$$

$$
\begin{aligned}
&(K_1 + G_{r,\text{dB}}(\Theta_1) - 2\log(r) - P_{r1,\text{dB}}) \\
&\qquad \times (G'_{r,\text{dB}}(\Theta_1) - G'_{r,\text{dB}}(\Theta_2)) = 0.
\end{aligned} \tag{A.5}
$$

(A.4) can give the range estimation (8). From (A.5), there are two cases, when $(K_1 + G_{r,\text{dB}}(\Theta_1) - 2\log(r) - P_{r1,\text{dB}}) = 0$ implies $(K_1 + G_{r,\text{dB}}(\Theta_2) - 2\log(r) - P_{r2,\text{dB}}) = 0$, so the angle estimation have the same expression as (3). Or $(G'_{r,\text{dB}}(\Theta_1) - G'_{r,\text{dB}}(\Theta_2)) = 0$ implies $G_r(\Theta_1)/G_r(\Theta_2)$ is local maximum or local minimum. Therefore, this gives us complete expression of (7).

B. Analysis of the Location Estimation Error With Additive Gaussian Noise

This section shows the variance of R caused by additive noise which can be calculated in similar analysis in Section II-B by applying (11) into (8). Considering the case of $P_{r,2} > P_{r,1}$ (to estimate the range errors from 0 to 45 degrees) where $n'_1 \triangleq (P_{r,1} + n_1^2)/P_{r,2}$; for the case of $P_{r,1} \geq P_{r,2}$, similar form can be obtained by replacing $n'_2 \triangleq P_{r,1}/(P_{r,2} + n_2^2)$. The overall variance of R is obtained as follows:

$$
\operatorname{var}(\hat{r}) \approx \frac{1}{2}\operatorname{var}(\hat{r} \mid P_{r,2} > P_{r,1}) + \frac{1}{2}\operatorname{var}(\hat{r} \mid P_{r,2} \leq P_{r,1}).
\tag{B.2}
$$

Furthermore, to obtain joint distribution of the location estimation, $f_{R,\Theta}$, Jacobian variable replacement is applied

to the joint distribution of $f_{np,1,np,2}$, which is equal to $f_{n_{p,1}}(n_1)f_{n_{p,2}}(n_2)$, as follows:

$$\begin{aligned} & f_{R,\Theta}(r,\theta) \\ & \quad = f_{n_{p,1}}\left(n_{p,1} = f_{p_r,n_1}(r,\theta)\right) \\ & \qquad \times f_{n_{p,2}}\left(n_{p,2} = f_{p_r,n_2}(r,\theta)\right)\left|\frac{\partial n_{p,1}\partial n_{p,2}}{\partial r\partial\theta}\right| \\ & \qquad = f_{n_{p,1}}\left(n_{p,1} = \frac{P_t G_t G_r(\theta)}{r^2} - p_{r,1}\right) \\ & \qquad \times f_{n_{p,2}}\left(n_{p,2} = \frac{P_t G_t G_r(\theta-\pi/2)}{r^2} - p_{r,2}\right) \\ & \qquad \times \left|\frac{G_r(\theta)G_r'(\theta-\pi/2) - G_r'(\theta)G_r(\theta-\pi/2)}{R}\right| \end{aligned} \tag{B.3}$$

where $f_{np,i}$ denotes the pdf of noise powers n_1^2 and n_2^2, and $P_{r,1}$ and $P_{r,2}$ are determined at a specific position.

ACKNOWLEDGMENT

The authors wish to thank the National Science Foundation for the support of this research and Intel for providing the sensor motes.

REFERENCES

[1] Y. Tirta, Z. Li, Y.-H. Lu, and S. Bagchi, "Efficient Collection of Sensor Data in Remote Fields Using Mobile Collectors," in *Proc. 13th IEEE Int. Conf. on Computer Communications and Networks (ICCCN'04)*, Oct. 11–13, 2004, pp. 515–519.

[2] J. Widmer, M. Mauve, H. Hartenstein, and H. Füßler, "Position-Based Routing in Ad-Hoc Wireless Networks," in *The Handbook of Ad Hoc Wireless Networks*. Boca Raton, FL: CRC Press, 2002, Mohammad Ilyas.

[3] J. Hightower and G. Borriello, Location Sensing Techniques Seattle, WA, Jul. 2001, Tech. Rep. Univ. of Washington CS Dept., UW-CSE-01-07-01.

[4] M. Vossiek, L. Wiebking, P. Gulden, J. Wieghardt, C. Hoffmann, and P. Heide, "Wireless Local Positioning," *IEEE Microwave Mag.*, vol. 4, pp. 77–86, Dec. 2003.

[5] L. Doherty, K. S. J. Pister, and L. El Ghaoui, "Convex position estimation in wireless sensor networks," in *IEEE Infocom 2001*, Anchorage, AK, Apr. 2001, vol. 3, pp. 1655–1663.

[6] Crossbow Technology Inc. [Online]. Available: http://www.xbow.com/Products/Product_pdf_files/Wireless_pdf/6020-0042-05_A_MICA2.pdf, MICA2 Datasheet online

[7] C.-L. Yang, S. Bagchi, and W. J. Chappell, "Location tracking with directional antennas in wireless sensor networks," in *Proc. IEEE MTT-S Int. Microwave Symp. Dig.*, Jun. 2005, pp. 131–134.

[8] K. Chintalapudi, A. Dhariwal, R. Govindan, and G. Sukhatme, "Ad-hoc localization using ranging and sectoring," in *IEEE Infocom*, Hong Kong, China, Mar. 2004, pp. 2662–2672.

[9] N. Malhotra, M. Krasniewski, C. Yang, S. Bagchi, and W. Chappell, "Location estimation in ad-hoc networks with directional antennas," in *25th Int. Conf. Distributed Computing Systems (ICDCS'05)*, Columbus, OH, Jun. 6–9, 2005.

[10] P. Bahl and V. N. Padmanabhan, "RADAR: An in-building RF-based user location and tracking system," in *IEEE Infocom 2000*, Tel Aviv, Isreal, Mar. 2000, vol. 2, pp. 775–784.

[11] K. Lorincz and M. Welsh, MoteTrack: A Robust, Decentralized Approach to RF-Based Location Tracking Tech. Rep. Harvard Univ. [Online]. Available: http://www.eecs.harvard.edu/~konrad/projects/motetrack/, TR-19-04,2004. MoteTrack project website:

[12] F. Aryanfar, S. Il-Koh, and K. Sarabandi, "Physics based ray-tracing propagation model for suburban areas," in *Proc. IEEE Antennas and Propagation Society Int. Symp.*, Jun. 22–27, 2003, vol. 4, pp. 903–906.

[13] S. Y. Seidel and T. S. Rapport, "914 MHz path loss prediction model for indoor wireless communications in multifloored buildings," *IEEE Trans. Antennas Propag.*, vol. 40, no. 2, pp. 207–217, Feb. 1992.

[14] MATLAB [Online]. Available: www.mathworks.com/

[15] N. Priyantha, A. Miu, H. Balakrishnan, and S. Teller, "The cricket compass for context-aware mobile applications," in *Proc. 7th ACM MOBICOM Conf.*, Jul. 2001.

[16] H. Karl and A. Willig, *Protocols and Architectures for Wireless Sensor Networks*, 1st ed. New York: Wiley, 2005.

[17] G. D. Durgin, T. S. Rappaport, and D. A. de Wolf, "New analytical models and probability density functions for fading in wireless communications," *IEEE Trans. Commun.*, vol. 50, pp. 1005–1015, Jun. 2002.

[18] E. K. P. Chong and S. H. Zak, *An Introduction to Optimization*, 2nd ed. New York: Wiley, 2001.

[19] T. K. Sarkar, Z. Ji, K. Kim, A. Medouri, and M. Salazar-Palma, "A survey of various propagation models for mobile communication," *IEEE Antennas Propag. Mag.*, vol. 45, no. 3, pp. 51–82, Jun. 2003.

[20] K. Whitehouse, "The Design of Calamari: An Ad-hoc Localization System for Sensor Networks," Master's thesis, Univ. California at Berkeley, CA, 2002.

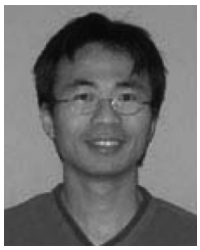

Chin-Lung Yang was born in Yung-Ling, Taiwan, R.O.C., in 1975. He received the B.S. and M.S. degrees in electrical engineering from National Tsing-Hua University and Communication Institute, National Taiwan University, in 1997 and 1999, respectively. He is currently working toward the Ph.D. degree in electrical and computing engineering at Purdue University, West Lafayette, IN.

His current research is focused on wireless sensor network, integrated RF front-ends, diversity design, wireless communication system, spread spectrum, and wireless channel characterization.

Saurabh Bagchi received the Ph.D. degree in computer science from the University of Illinois at Urbana-Champaign. His Ph.D. dissertation was on error detection protocols in distributed systems and was implemented in a fault-tolerant middleware system called Chameleon.

In August 2002, he joined the School of Electrical and Computer Engineering at Purdue University, West Lafayette, IN, as an Assistant Professor. He is a member of the Dependable Computing Systems Lab where he carries out research in design and implementation of dependable distributed systems and sensor networks.

William J. Chappell (S'98–M'02) received the B.S.E.E., M.S.E.E., and Ph.D. degrees from the University of Michigan at Ann Arbor, in 1998, 2000, and 2002, respectively.

He is currently an Assistant Professor with the Electrical and Computer Engineering Department, Purdue University, West Lafayette, IN, where he is also a member of the Birck Nanotechnology Center and the Center for Wireless Systems and Applications. His research focuses on silicon micromachining, polymer formation, and low-loss ceramics for high-frequency circuits and antennas. His research interests also include rapid prototyping, free-form fabrication, and small-scale formation of electrically functioning ceramic and polymer passive components. He also oversees projects investigating RF design for wireless sensor networks, chemical sensors, and electrotextiles.

Dr. Chappell was the recipient of the 2004 Joel Spira Outstanding Educator Award and has been designated as a Teacher for Tomorrow in his department. He is a reviewer for the IEEE TRANSACTIONS ON ANTENNAS AND PROPAGATION.